

Design and development of a fluorescent probe for monitoring hydrogen peroxide using photoinduced electron transfer

Nobuaki Soh,^a Osamu Sakawaki,^a Koji Makihara,^a Yuka Odo,^a Tuyoshi Fukaminato,^a
Tsuyoshi Kawai,^b Masahiro Irie^a and Toshihiko Imato^{a,*}

^aDepartment of Applied Chemistry, Graduate School of Engineering, Kyushu University, 6-10-1, Hakozaki, Higashi-ku, Fukuoka 812-8581, Japan

^bResearch and Education Center for Materials Science, Nara Institute of Science and Technology, 8916-5, Takayama, Ikoma, Nara 630-0192, Japan

Received 30 October 2004; revised 11 November 2004; accepted 12 November 2004
Available online 2 December 2004

Abstract—A novel fluorescent probe, 7-hydroxy-2-oxo-*N*-(2-(diphenylphosphino)ethyl)-2*H*-chromene-3-carboxamide (DPPEA-HC) was developed for use in monitoring hydrogen peroxide (H₂O₂) production. DPPEA-HC, which consists of a diphenylphosphine moiety and a 7-hydroxycoumarin moiety, reacts with H₂O₂ to form DPPEA-HC oxide, which is analogous to the reaction of triphenylphosphine with hydroperoxides such as H₂O₂ to form triphenylphosphine oxide. Photoinduced electron transfer (PET) was applied in the design of DPPEA-HC. Since the diphenylphosphine moiety and the 7-hydroxycoumarin moiety would act as the PET donor and the acceptor, respectively, it would be expected that DPPEA-HC would rationally cancel the PET process via the formation of DPPEA-HC oxide, based on the calculated energy levels of the donor and the acceptor moieties using the B3LYP/6-31G**//AM1 method. The fluorescence intensity of DPPEA-HC increased on the addition of a H₂O₂ solution in 100 mM sodium phosphate buffer (pH 7.4), as predicted from the energy level calculation and a good correlation between increase in the fluorescence of DPPEA-HC and the concentration of H₂O₂ was observed. DPPEA-HC was also fluoresced by H₂O₂, which was enzymatically produced in xanthine/xanthine oxidase/superoxide dismutase (XA/XOD/SOD) system. The increase in the fluorescence of DPPEA-HC in the presence of H₂O₂ immediately ceased on the addition of catalase (CAT), which catalyzes the disproportionation of H₂O₂. In addition, DPPEA-HC was found to have a much higher selectivity for H₂O₂ and a greater resistance to autoxidation than 2',7'-dichlorodihydrofluorescein (DCFH). Time-resolved fluorescence measurements of DPPEA-HC and DPPEA-HC oxide confirmed that the fluorescence off/on switching mechanism of DPPEA-HC is based on the PET on/off control.

© 2004 Elsevier Ltd. All rights reserved.

1. Introduction

Reactive oxygen species (ROS) are thought to play a key role not only in pathological conditions and chronic diseases but also in certain normal physiological processes.¹ Among other ROS, hydrogen peroxide (H₂O₂) is vasoactive and has been detected under various pathophysiological conditions, including inflammation,² hypoxia-reoxygenation,³ and the deficiency of a co-factor for nitric oxide (NO) synthesis.⁴ Recent studies have suggested that H₂O₂ functions as an endothelium-derived hyperpolarizing factor⁵ in small arteries and acti-

vates potassium channel opening in large cerebral arteries.⁶ Although a number of reports have documented the significance of H₂O₂ in biological systems, the mechanism of its action is poorly understood because of the limited availability of detection methods.

Detection methods using fluorescent probes are quite useful for clarifying the functions of a target biomolecule in biological systems because temporal and spatial information concerning the target molecule can be obtained with a high degree of sensitivity in vivo cellular systems.⁷ Therefore, various fluorescent probes for monitoring ROS such as NO,⁸ singlet oxygen,⁹ and hydroxyl radical (·OH)¹⁰ have been developed in recent years. However, only a few fluorescent probes for H₂O₂ have been reported. Though 2',7'-dichlorodihydrofluorescein (DCFH) and dihydrorhodamine 123 (DHR123) can be used as a H₂O₂ probe,¹¹ they tend to react with a variety

Keywords: Hydrogen peroxide; Fluorescent probe; Reactive oxygen species; Photoinduced electron transfer.

*Corresponding author. Tel.: +81 92 642 3569; fax: +81 92 642 4134; e-mail: imato@cstf.kyushu-u.ac.jp

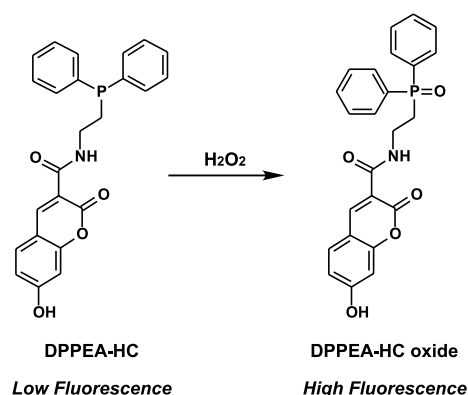
of ROS, and furthermore, the former probe is easily auto-oxidized and the fluorescence intensity of the probe spontaneously increases upon exposure to light.¹² Therefore, DCFH and DHR123 should be considered as probes for detecting a broad range of oxidizing reactions that may be increased during intracellular oxidative stress. A europium-ion-based luminescent sensing probe was also reported for detecting H_2O_2 .¹³ Unfortunately, however, the luminescence is affected by phosphate and citrate. If a probe with a higher selectivity for H_2O_2 and a better stability against autooxidation could be developed, the biological roles of H_2O_2 would be expected to be clarified greatly.

We wish to report herein on the design and development of a novel fluorescent probe, 7-hydroxy-2-oxo-*N*-(2-(diphenylphosphino)ethyl)-2*H*-chromene-3-carboxamide (DPPEA-HC) for monitoring H_2O_2 . For the design of the proposed probe, a photoinduced electron transfer (PET) mechanism was utilized because recent studies^{8c,9c,14,15} support the effectiveness of the PET-controlled fluorescence off/on switching mechanism for the rational design of fluorescent probes. The performance of DPPEA-HC was evaluated with respect to the detection ability and the selectivity for H_2O_2 . A time-resolved fluorescence study of the probe was also carried out, to permit a more comprehensive discussion of the PET-controlled fluorescence off/on switching mechanism.

2. Results and discussion

2.1. Design of novel fluorescent probe for H_2O_2 based on the control of PET process

One of the most important factors in the design of a fluorescent probe for a target molecule involves the selection of a specific reaction that can be used as the basis for selectively detecting the analyte. We concluded that a reaction of triphenylphosphine with hydroperoxides is a suitable reaction that would permit the design of a novel fluorescent probe for H_2O_2 . Triphenylphosphine was reported to react with hydroperoxides such as H_2O_2 to produce triphenylphosphine oxide.¹⁶ In the reaction, a lone electron pair of the phosphorus atom in triphenylphosphine would be lost as the result of the formation of triphenylphosphine oxide. Therefore, a phosphine compound, in which an appropriate fluorophore is substituted for a phenyl group of triphenyl phosphine (i.e., a diphenyl phosphine containing a fluorophore) would permit the fluorescence intensity to be increased when the phosphine compound reacts with H_2O_2 because the PET derived from the lone electron pair of the phosphorus atom to the fluorophore may be cancelled in the reaction. In fact, diphenyl-1-pyrenylphosphine (DPPP) has been reported to react with hydroperoxides to form DPPP oxide, resulting in an increase in fluorescence intensity.¹⁷ However, DPPP is a highly hydrophobic compound and, thus, is not suitable for the analysis of H_2O_2 in aqueous media. We therefore designed a more hydrophilic diphenylphosphine derivative, DPPEA-HC, as a novel fluorescent probe for determining H_2O_2 in aqueous media (Scheme 1). Recently,



Scheme 1. Reaction of DPPEA-HC with H_2O_2 .

4-(2-diphenylphosphinoethylamino)-7-nitro-2,1,3-benzoxadiazole was reported as a PET reagent for hydroperoxides.¹⁵ The reagent quantitatively reacts with *tert*-butyl hydroperoxide or cumene hydroperoxide to increase its fluorescence intensity in organic solvents, however, the reactivity of the reagent with H_2O_2 in an aqueous media has not yet been reported.

For the design of DPPEA-HC, we introduced the rational method for designing a PET-type fluorescent probe, which was proposed by Nagano and Urano et al.^{8c,9c,14} If DPPEA-HC is divided into two parts, namely, a diphenylphosphine moiety (donor) and a 7-hydroxycoumarin moiety (acceptor) (Fig. 1a), a well-grounded prediction of fluorescence off/on switching based on the PET process would be possible using the method. PET is a widely accepted mechanism for fluorescence quenching where an electron transfer from a PET donor to the excited acceptor diminishes the fluorescence of the acceptor.¹⁸ If the highest occupied molecular orbital (HOMO) energy level of the donor is sufficiently high for electron transfer to the excited acceptor, the value of the quantum efficiency of fluorescence (ϕ) will be small, that is, fluorescent derivatives with high ϕ values must have an electron donor moiety with low HOMO energy levels (Fig. 1b). The HOMO energy levels of methyldiphenylphosphine (the donor in DPPEA-HC) and methyldiphenylphosphine oxide (the donor in DPPEA-HC oxide) were estimated to be -8.33 and -9.95 eV, based on B3LYP/6-31G*//AM1 calculations. Therefore, if the energy level of an acceptor moiety in the excited state is located between the HOMO energy levels of methyldiphenylphosphine and methyldiphenylphosphine oxide, DPPEA-HC would cancel the PET process when DPPEA-HC reacts with H_2O_2 to form DPPEA-HC oxide. For the rational design of PET-type fluorescent probes with a fluorescein structure, Nagano and Urano et al. evaluated the fluorescence off/on threshold of fluorescein derivatives by considering both the calculated HOMO energy levels of the donor moiety in various fluorescein derivatives (donor moiety: benzoic acid moiety, acceptor moiety: xanthene ring) and the values of the quantum efficiency of the fluorescence of the fluorescein derivatives, which were obtained by experimental fluorometric analysis.^{9c}

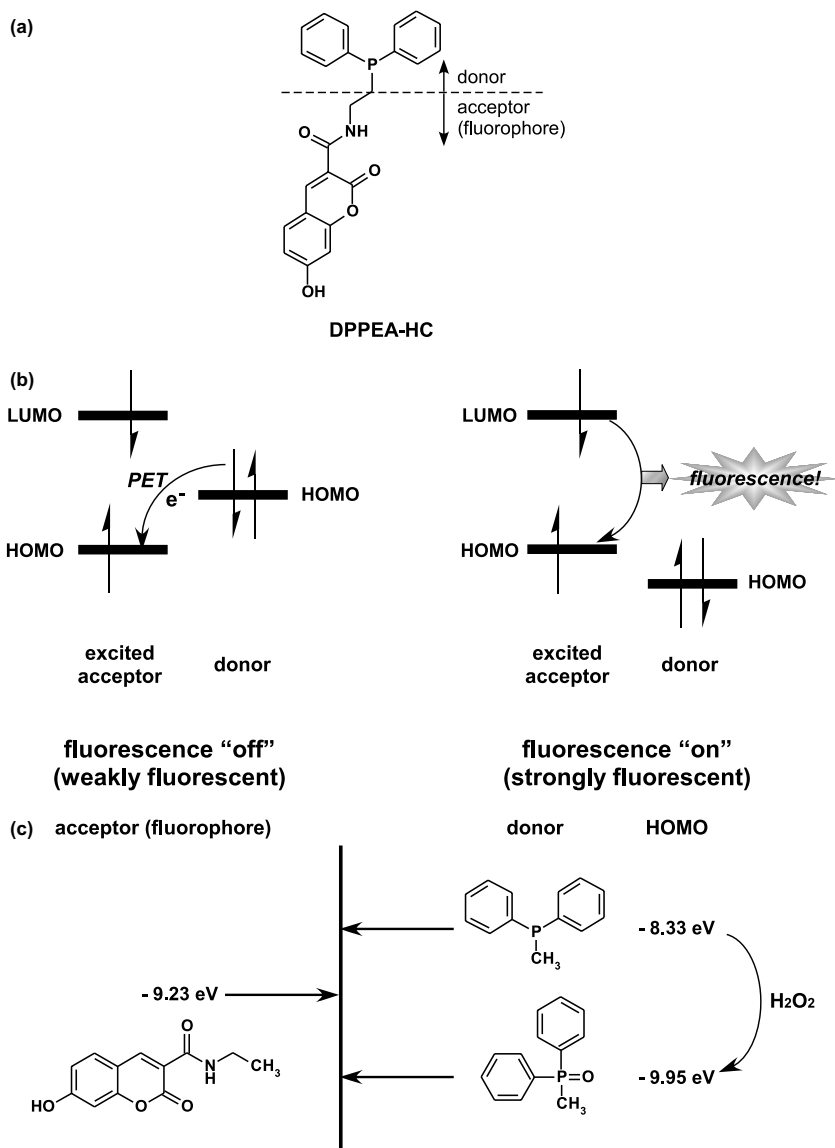
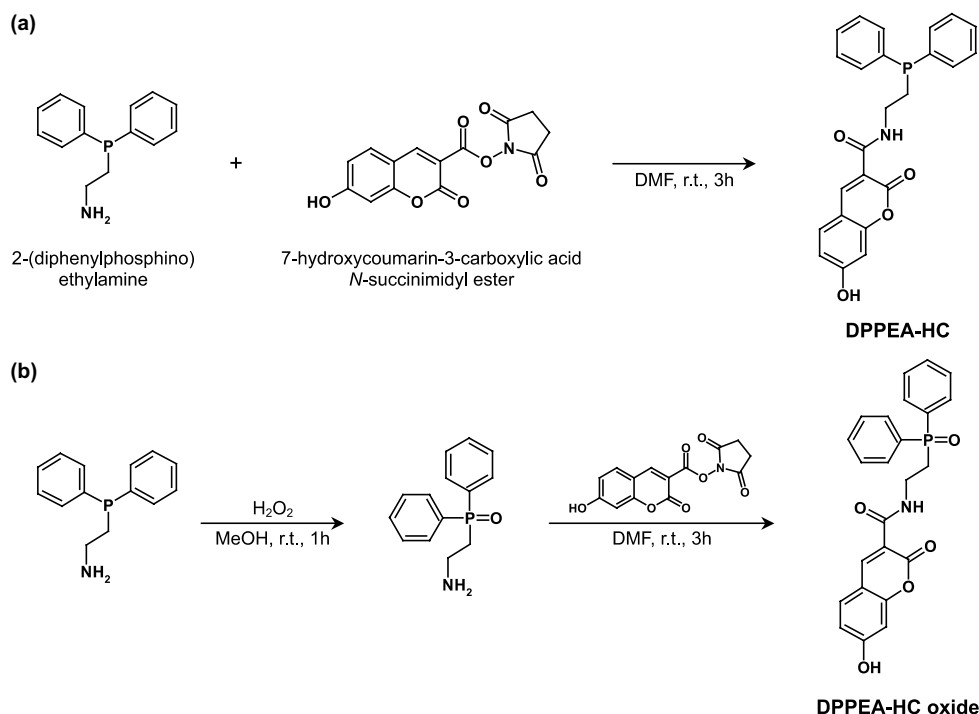


Figure 1. Design of a novel fluorescent probe for H_2O_2 based on the control of PET process: (a) the structure of DPPEA-HC divided into two parts, the PET donor and the acceptor (fluorophore); (b) illustration of the thermodynamic situation for the fluorescence off/on switching based on control of the PET process; (c) HOMO energy levels of donor (methyl-diphenylphosphine, methyl-diphenylphosphine oxide), and the energy level of acceptor (*N*-ethyl-7-hydroxy-2-oxo-2*H*-chromene-3-carboxamide) at excited state, obtained from B3LYP/6-31G**/AM1 calculations.

In this study, we evaluated the fluorescence off/on threshold of the H_2O_2 probe from the calculated energy level of the excited acceptor. The energy level of *N*-ethyl-7-hydroxy-2-oxo-2*H*-chromene-3-carboxamide (acceptor in DPPEA-HC or DPPEA-HC oxide) in the excited state was estimated to be -9.23 eV , based on B3LYP/6-31G**/AM1 calculations. Therefore, the HOMO energy level of methyl-diphenylphosphine (-8.33 eV), the donor moiety of DPPEA-HC, is sufficiently high to induce the PET process to the excited acceptor, on the other hand, the HOMO energy level of methyl-diphenylphosphine oxide (-9.95 eV), the donor moiety of DPPEA-HC oxide, is sufficiently low to permit cancellation of the PET process (Fig. 1c). Thus, it would be rationally expected that DPPEA-HC would react with H_2O_2 to cancel PET process and increase the fluorescence intensity.

2.2. Synthesis of DPPEA-HC and its detection ability for H_2O_2

DPPEA-HC and DPPEA-HC oxide were synthesized from 2-(diphenylphosphino)ethylamine and 7-hydroxy-coumarin-3-carboxylic acid *N*-succinimidyl ester, as shown in Scheme 2. Figure 2 shows fast atom bombardment (FAB) mass spectra of DPPEA-HC, DPPEA-HC oxide, and DPPEA-HC after reaction with a sufficient amount of H_2O_2 . The peaks for DPPEA-HC ($m/z = 418$) and DPPEA-HC oxide ($m/z = 434$) can be readily assigned from the calculated values ($[\text{M}+\text{H}]^+ = 418$ for DPPEA-HC, 434 for DPPEA-HC oxide), respectively, and the peak of sample solution of DPPEA-HC, after reaction with a sufficient amount of H_2O_2 in aqueous media ($m/z = 434$), is in good agreement with that of DPPEA-HC oxide synthesized. This result clearly



Scheme 2. Synthetic schemes for (a) DPPEA-HC; (b) DPPEA-HC oxide.

confirms that DPPEA-HC reacted with H₂O₂ to yield DPPEA-HC oxide in aqueous media.

DPPEA-HC was next applied to the detection of H₂O₂ in 100 mM sodium phosphate buffer (pH 7.4). As expected from the previous section, the fluorescence intensity of DPPEA-HC increased with an increase in the concentration of added H₂O₂, and was saturated at concentrations higher than 50 μ M, where 99% of DPPEA-HC is calculated to be reacted with H₂O₂ to form DPPEA-HC oxide from the fluorescence intensity of DPPEA-HC oxide, which was synthesized in this work (Fig. 3). Figure 4 shows the time courses for the fluorescence intensity of DPPEA-HC after the addition of various concentrations of H₂O₂. In this case, the fluorescence intensity of DPPEA-HC was normalized by the intensity before the addition of H₂O₂. The fluorescence intensity of DPPEA-HC increased as a function of H₂O₂ concentration. From the results shown in Figures 3 and 4, DPPEA-HC was able to detect μ M level of H₂O₂.

To confirm that the fluorescence changes of DPPEA-HC were caused by H₂O₂, catalase (CAT), which acts as a scavenger of H₂O₂ by catalyzing the disproportionation of H₂O₂ into water and molecular oxygen,¹⁹ was added to a solution of DPPEA-HC, in which the reaction of DPPEA-HC with H₂O₂ was proceeding. As can be seen from Figure 5, the increase in fluorescence intensity was completely suppressed by the addition of CAT. This result confirms that the fluorescence changes in DPPEA-HC shown in Figures 3 and 4 are due to H₂O₂.

DPPEA-HC was also applied to the detection of H₂O₂ generated in a xanthine/xanthine oxidase/superoxide dis-

mutase (XA/XOD/SOD) system²⁰ xanthine oxidase (XOD) catalyzes the incorporation of oxygen (derived from water) into xanthine (XA) to yield uric acid, superoxide anion (O₂^{•−}) and H₂O₂. Superoxide dismutase (SOD) catalyzes the disproportionation of O₂^{•−} to yield H₂O₂.²¹ Thus, H₂O₂ is generated enzymatically in the XA/XOD/SOD system. As shown in Figure 6, the fluorescence intensity of a DPPEA-HC solution in the presence of XA and SOD increased on the addition of XOD (XA/XOD/SOD system) as well as the case, in which H₂O₂ was added directly to the DPPEA-HC solution (Figs. 3 and 4). In addition, the increase in fluorescence was distinctly suppressed on the addition of CAT (XA/XOD/SOD/CAT system) as well as the case shown in Figure 5. The results, showing that DPPEA-HC functioned, even in an enzymatic system, strongly support the conclusion that the probe would be applicable in biological systems.

Table 1 shows the increment of the fluorescence intensity of DPPEA-HC in various ROS generating systems. The values were calculated by subtracting the experimental values of fluorescence intensities of DPPEA-HC before the addition of these ROS from those of DPPEA-HC after the addition of the ROS. The data for DCFH, taken from literature,^{10c} are also listed in Table 1, for comparison. As shown in Table 1, DPPEA-HC has a much higher selectivity for H₂O₂ than DCFH. It is particularly noteworthy that the fluorescence of DPPEA-HC was not influenced significantly by peroxy-nitrite (ONOO[−]), [•]OH, and alkylperoxyl radical (ROO[•]), while the fluorescence of DCFH was greatly increased in the presence of these ROS. In the ONOO[−] generating system, a commercial ONOO[−] solution, in which excess H₂O₂ is removed with manganese dioxide,

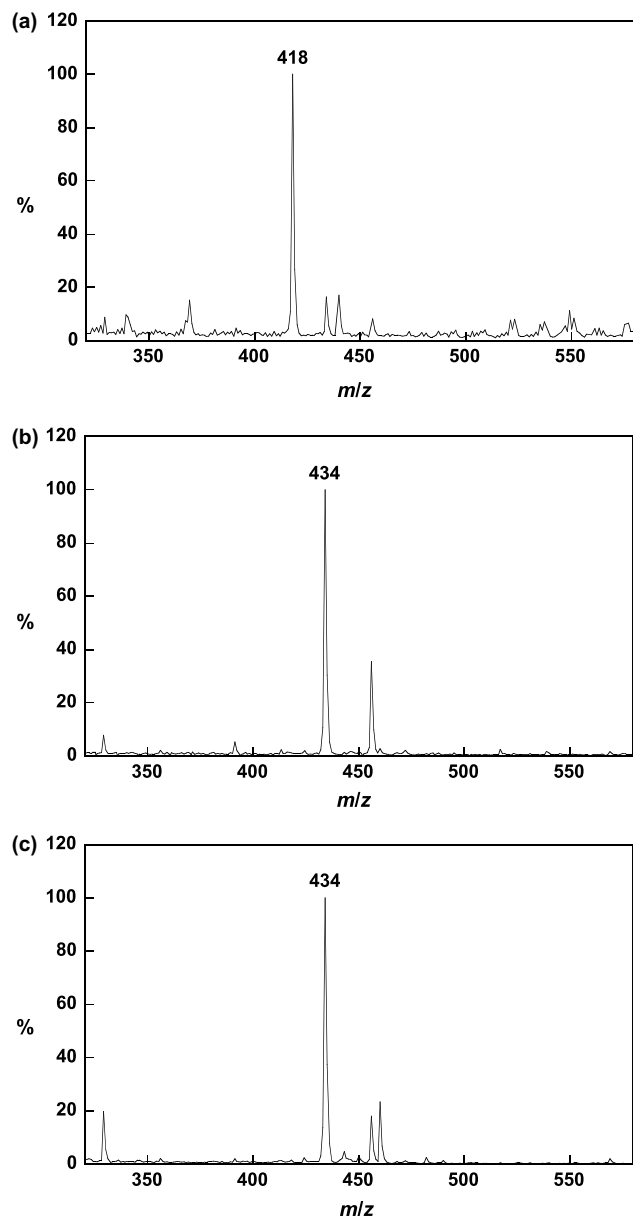


Figure 2. FAB mass spectra of (a) DPPEA-HC: (b) DPPEA-HC oxide: (c) DPPEA-HC, after reaction with a sufficient amount of H₂O₂.

was used. In the $\cdot\text{OH}$ generating system, the molar ratio of $\text{Fe(II)}:\text{H}_2\text{O}_2$ in the Fenton reagent is 1:1. Therefore, it would be expected that insignificant amount of H₂O₂ exists in both systems and the results in these systems would reflect the effects of ONOO⁻ and $\cdot\text{OH}$ themselves. In addition, the fluorescence of DPPEA-HC increased negligibly due to autoxidation upon illumination, whereas DCFH was extensively autoxidized, resulting in a dramatic increase in fluorescence intensity. Unexpectedly, DPPEA-HC fluoresced with O₂^{•-} and NO as with H₂O₂. Although the reason for this is not clear at this stage, it is possible that DPPEA-HC reacted with these radicals as well as H₂O₂ to form DPPEA-HC oxide. However, concerning NO, since many fluorescent probes that perform well have been reported,⁸ interference from NO for the biological imaging of H₂O₂ using

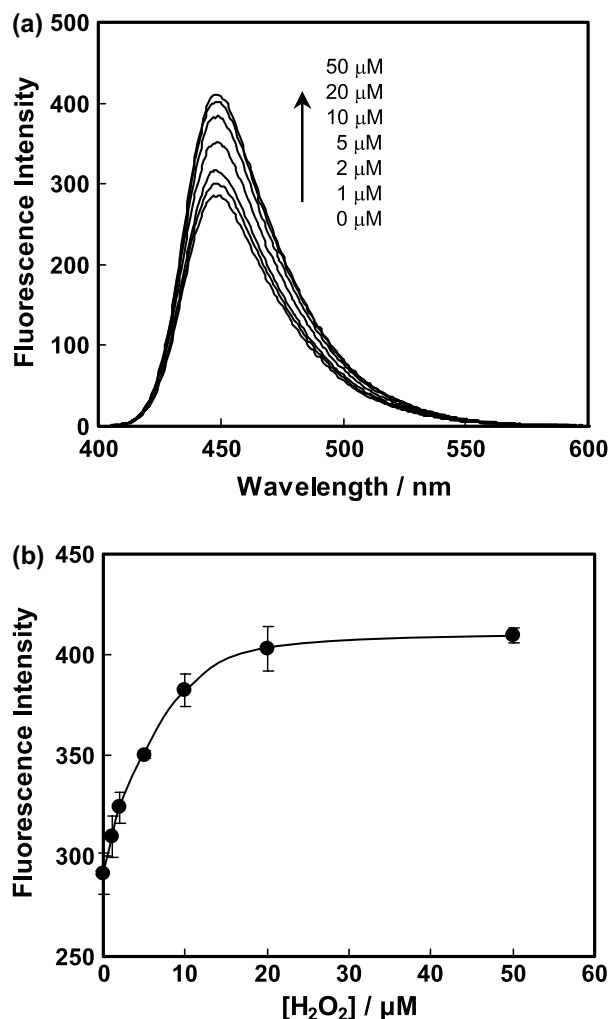


Figure 3. (a) Emission spectra (representative data are shown): (b) fluorescence intensity at 449 nm (data are the mean \pm SD, $n = 3$) for DPPEA-HC at 37°C in 100 mM sodium phosphate buffer (pH 7.4) in the presence of various concentration of H₂O₂ ranging from 0 to 50 μM with excitation at 396 nm. The emission spectra were obtained 30 min after the addition of H₂O₂ to a 5 μM DPPEA-HC solution under aerobic conditions. The denoted values for H₂O₂ concentration are cumulative concentrations.

DPPEA-HC may be therefore deduced if such an NO fluorescent probe is applied together with DPPEA-HC for the imaging of H₂O₂. Moreover, the interference from O₂^{•-} may be also differentiated from H₂O₂, for example, by utilizing SOD, which is thought to internalize in living cells through endocytosis.²² Thus, DPPEA-HC appears to be superior to DCFH, an ordinary probe for H₂O₂, from the standpoint of both selectivity to H₂O₂ against other ROS and resistance to autoxidation. Thus, we believe that DPPEA-HC represents an attractive novel fluorescent probe for detecting H₂O₂.

2.3. Fluorescence parameters of DPPEA-HC and PET-controlled fluorescence off/on switching mechanism

In this section, the fluorescence parameters of DPPEA-HC were evaluated, to permit the PET-controlled fluorescence off/on switching mechanism of DPPEA-HC

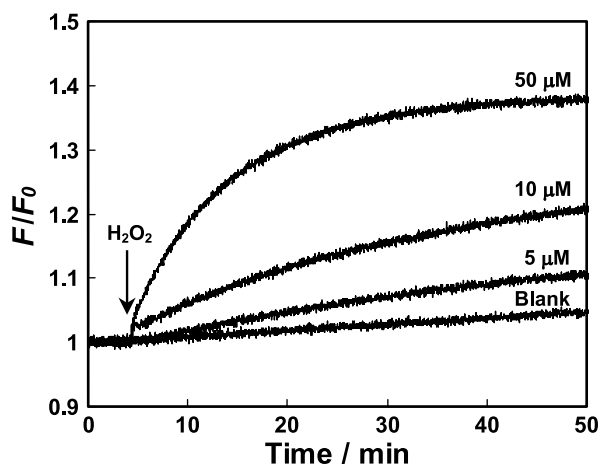


Figure 4. Time courses of relative fluorescence intensity (F/F_0) of DPPEA-HC depending on H_2O_2 at $37^\circ C$ in 100mM sodium phosphate buffer (pH 7.4). A solution of H_2O_2 (final 0–50 μM) was added at the point indicated by an arrow. F_0 and F denote the fluorescence intensity at 449nm before and after the addition of H_2O_2 , respectively, with excitation at 396nm.

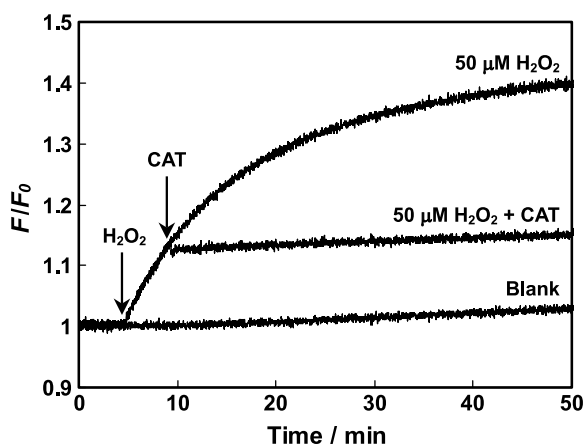


Figure 5. Effect of catalase (CAT) on fluorescence changes in DPPEA-HC. CAT (final 90 units/mL) was added to 100mM sodium phosphate buffer (pH 7.4), which contains 5 μM DPPEA-HC and 50 μM H_2O_2 . The fluorescence intensity (F_0 : initial fluorescence intensity, F : fluorescence intensity) was determined at 449nm with excitation at 396 nm. The added points of H_2O_2 and CAT were indicated by arrows.

that we designed at the first stage to be discussed. The absorbance and fluorescence properties of DPPEA-HC and DPPEA-HC oxide are summarized in Table 2. The formation of DPPEA-HC oxide from DPPEA-HC led to little change in the absorbance maxima but increased the value for the quantum efficiency of fluorescence, ϕ , a characteristic feature of PET-type probes. The increase in with the formation of DPPEA-HC oxide strongly supports the hypothesis that the fluorescence off/on switching of DPPEA-HC is based on the PET mechanism. Figure 7 shows time-resolved fluorescence decay curves for DPPEA-HC and DPPEA-HC oxide. The lifetimes of DPPEA-HC and DPPEA-HC oxide, as evaluated from the slopes of the decay curves in Figure 7, were determined to be 2.8 and 3.8 ns, respectively.

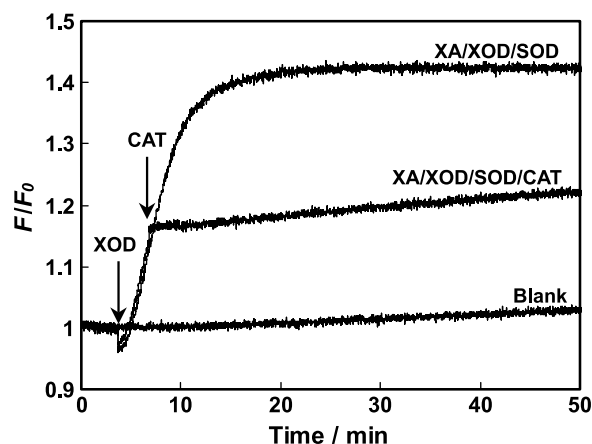


Figure 6. Time courses for the relative fluorescence intensity (F/F_0) of DPPEA-HC in the enzymatic XA/XOD/SOD system and the XA/XOD/SOD/SOD/CAT system at $37^\circ C$ in 100mM sodium phosphate buffer (pH 7.4). In the XA/XOD/SOD system, XOD (final 0.05 units/mL) was added to a 5 μM DPPEA-HC solution with 100 μM XA and 100 units/mL SOD. In the XA/XOD/SOD/SOD/CAT system, CAT (final 90 units/mL) was further added after the addition of the same concentration of XOD. The fluorescence intensity (F_0 : initial fluorescence intensity, F : fluorescence intensity) was determined at 449nm with excitation at 396nm. The added points of XOD and CAT were indicated by arrows.

Table 1. Fluorescence increase in DPPEA-HC after reaction with various ROS

ROS	DPPEA-HC	DCFH ⁱ
$H_2O_2^a$	137	190
$ONOO^-^b$	11	6600
$-OCl^c$	<1	86
$\cdot OH^d$	8	7400
ROO^e	46	710
$O_2^{\cdot -f}$	126	67
NO^g	126	150
Autooxidation ^h	27	2000

Various ROS were generated in a DPPEA-HC solution (final 5 μM , 0.2% DMSO as a co-solvent) and the mixture was stirred at $37^\circ C$ for 60min. The fluorescence intensity was determined at 449nm with excitation at 396nm.

^a H_2O_2 (final 50 μM) was added to 100mM sodium phosphate buffer (pH 7.4).

^b $ONOO^-$ (final 1.5 μM) was added to 100mM sodium phosphate buffer (pH 7.4).

^c $NaOCl$ (final 1.5 μM) was added to 100mM sodium phosphate buffer (pH 7.4).

^d Ferrous perchlorate and H_2O_2 (final 50 μM , each) were added to 10mM Tris-HCl buffer (pH 7.4).

^e 2,2'-Azobis(2-amidinopropane)dihydrochloride (final 50 μM) was added to 100mM sodium phosphate buffer (pH 7.4).

^f KO_2 (final 50 μM) was added to 100mM sodium phosphate buffer (pH 7.4).

^g NOC7 (final 50 μM) was added to 100mM sodium phosphate buffer (pH 7.4).

^h A dye solution was placed under a fluorescent lamp for 2.5h.

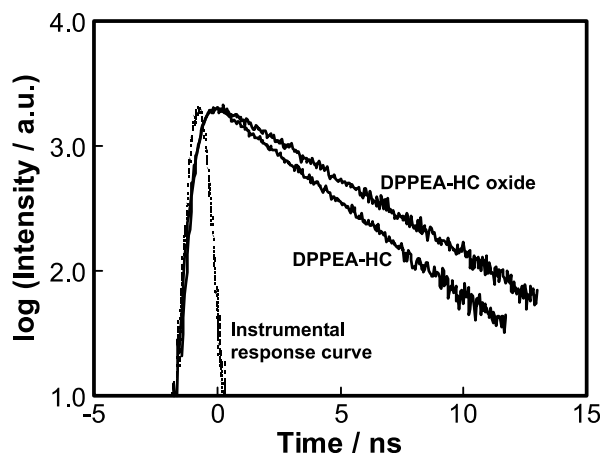
ⁱ Fluorescence increase of DCFH was also listed in Table 1 for reference. The data for DCFH were extracted from Ref. 10c. A part of the experimental conditions for DCFH are different from that for DPPEA-HC, for example, the slit width (2.5 nm for both excitation and emission were used) in fluorometric analysis, concentrations of fluorescent probe and ROS (basically twice the concentrations were used, such as 10 μM dye (DCFH), 100 μM H_2O_2 , or 3 μM $ONOO^-$).

Table 2. Absorbance and fluorescence properties of DPPEA-HC and DPPEA-HC oxide^a

Compound	Absorbance maximum (nm)	Extinction coefficient ($\times 10^4 \text{ M}^{-1} \text{ cm}^{-1}$)	Emission maximum (nm)	Relative quantum yield ^b
DPPEA-HC	403	3.4	449	0.58
DPPEA-HC oxide	405	3.1	446	0.82

^a All data were measured in 100 mM sodium phosphate buffer at pH 7.4 (0.2% DMSO as a cosolvent).

^b Quantum yield of fluorescence was determined using that of 7-hydroxycoumarin (0.76) in 100 mM sodium phosphate buffer at pH 7.4 as a standard.

**Figure 7.** Time-resolved fluorescence decay curves for DPPEA-HC and DPPEA-HC oxide (5 μM , respectively) at room temperature in 100 mM sodium phosphate buffer (pH 7.4) under excitation with 362 nm light.

The longer lifetime of DPPEA-HC oxide than that of DPPEA-HC indicates that the PET process was suppressed in the case of DPPEA-HC oxide, different from DPPEA-HC. The lifetime of DPPEA-HC after the addition of a sufficient amount of H_2O_2 to the aqueous solution (5 μM DPPEA-HC, 3 mM H_2O_2) was determined to be 3.7 ns, similar to that of DPPEA-HC oxide (3.8 ns). This result clearly demonstrates that the fluorescence off/on switching of DPPEA-HC triggered by the addition of H_2O_2 is due to the PET on/off switching mechanism.

The rate constant for the forward electron transfer (k_{et}) in DPPEA-HC from donor to acceptor (see Fig. 1b, left) can be calculated using the following equation²³

$$k_{\text{et}} = 1/\tau - 1/\tau_{\text{ref}} \quad (1)$$

where τ and τ_{ref} denote the fluorescence lifetime of DPPEA-HC and DPPEA-HC oxide, respectively. The k_{et} value in DPPEA-HC was determined to be $9.4 \times 10^7 \text{ s}^{-1}$ from Eq. 1 by using the fluorescence lifetimes of DPPEA-HC and DPPEA-HC oxide. On the other hand, the k_{et} value for DPPEA-HC can be also calculated using the following equation^{14,23}

$$\phi_{\text{ref}}/\phi = 1 + k_{\text{et}}/k_{\text{ref}} \quad (2)$$

where ϕ and ϕ_{ref} denote the quantum efficiencies of fluorescence of DPPEA-HC and DPPEA-HC oxide, respectively, and $k_{\text{ref}} = 1/\tau_{\text{ref}}$, which was determined to be $2.6 \times 10^8 \text{ s}^{-1}$. The k_{et} value calculated using Eq. 2 was determined to be $1.1 \times 10^8 \text{ s}^{-1}$, a value that is almost the same as the k_{et} value ($9.4 \times 10^7 \text{ s}^{-1}$) determined from Eq. 1. This result indicates that the obtained k_{et} values represent reasonable rate constants for the forward electron transfer in DPPEA-HC.

3. Conclusion

In conclusion, we report on the design and development of a novel fluorescent probe for the detection of H_2O_2 by utilizing the fluorescence off/on switching mechanism, based on the PET on/off control. The fluorescence intensity of DPPEA-HC increased with an increase in the concentration of H_2O_2 , as expected from the calculated energy levels of the donor and acceptor moieties in DPPEA-HC and DPPEA-HC oxide using the B3LYP/6-31**/AM1 method. DPPEA-HC was superior to DCFH in terms of both selectivity for H_2O_2 and resistance to autooxidation, therefore, DPPEA-HC would be expected to be a novel and useful fluorescent probe for H_2O_2 . The biological imaging of H_2O_2 in living cells with DPPEA-HC would be achieved by a microinjection method or by converting DPPEA-HC to ester derivatives, which would be able to permeate through the cell membrane. We hope that our report will lead to a better understanding of biological roles of H_2O_2 in the future.

4. Experimental

4.1. Materials

2-(Diphenylphosphino)ethylamine, 7-hydroxycoumarin-3-carboxylic acid *N*-succinimidyl ester, and 7-hydroxycoumarin-3-carboxylic acid were purchased from Fluka. Hydrogen peroxide and sodium hypochlorite solution were purchased from Kishida Chemical Co. Ltd. Xanthine (XA), xanthine oxidase (XOD), superoxide dismutase (SOD), and catalase (CAT) were purchased from Sigma. Peroxynitrite solution, 1-hydroxy-2-oxo-3-(*N*-methyl-3-aminopropyl)-3-methyl-1-triazene (NOC7) were purchased from Dojindo Laboratories. Potassium superoxide (KO_2) was purchased from Acros. 2,2-Azobis(2-amidinopropane)dihydrochloride were purchased from Wako Pure Chemical Industries Co. Ltd. Other materials were of the highest grade available and used without further purification.

4.2. Instruments

^1H NMR spectra were recorded on an AC-250P spectrometer (Bruker). Mass spectra were obtained with a JMS mate II (JEOL). UV-vis spectra were obtained on a V-560 UV/Vis spectrophotometer (JASCO). Steady-state fluorescence spectroscopic studies were performed on a RF-5300PC (Shimadzu). Fluorescence lifetimes were measured with a time-resolved spectrofluorometer (Hamamatsu Photonics C4334-01, C5094, and

C4792) excited with a pulsed N₂ laser and a laser system (Laser Photonics, Inc., LN-203C and LD2S).

4.3. Synthesis of DPPEA-HC

2-(Diphenylphosphino)ethylamine (52.0 mg, 0.23 mmol) and 7-hydroxycoumarin-3-carboxylic acid *N*-succinimidyl ester (63.9 mg, 0.21 mmol) were dissolved in 0.3 mL of absolute DMF under a N₂ atmosphere, and the solution was stirred at room temperature for 3 h. The reaction mixture was evaporated and the crude compound was purified by thin layer chromatography on silica gel 60 plates (Merck) eluting with CHCl₃/MeOH = 85/15, and extracting with CHCl₃/MeOH = 60/40. The purification process was carried out by two times to afford a yellow powder (25 mg, yield 28%). ¹H NMR (DMSO-*d*₆): δ 2.39 (t, 2H, *J* = 7.5 Hz); 3.36–3.48 (m, 3H); 6.73 (s, 1H); 6.82 (d, 1H, *J* = 8.3 Hz); 7.26–7.47 (m, 10H); 7.76 (d, 1H, *J* = 8.6 Hz); 8.72 (s, 1H); 8.78 (t, 1H, *J* = 5.42 Hz). HRMS (FAB⁺): calcd for [M+H]⁺, 418.1208; found, 418.1208. Mp: 167–169 °C.

4.4. Synthesis of DPPEA-HC oxide

2-(Diphenylphosphino)ethylamine (38.1 mg, 0.17 mmol) was dissolved in 0.2 mL of MeOH, then 100 μL of an H₂O₂ solution (1 mmol) was added, and the reaction mixture was stirred at room temperature for 1 h. The resulting mixture was evaporated and dissolved in 0.3 mL of absolute DMF, and 7-hydroxycoumarin-3-carboxylic acid *N*-succinimidyl ester (31.4 mg, 0.1 mmol) was then added. The reaction mixture was stirred at room temperature for 3 h. The mixture was evaporated and the crude compound was purified by thin layer chromatography on silica gel 60 plates (Merck) eluting with CHCl₃/MeOH = 85/15, and extracting with CHCl₃/MeOH = 60/40 to afford a yellowish brown powder (20.3 mg, yield 45%). ¹H NMR (DMSO-*d*₆): δ 2.69 (t, 2H, *J* = 10.4 Hz); 3.39–3.62 (m, 3H); 6.72 (s, 1H); 6.82 (d, 1H, *J* = 8.6 Hz); 7.42–7.50 (m, 6H); 7.59–7.77 (m, 5H); 8.67 (s, 1H); 8.78 (t, 1H, *J* = 5.3 Hz). HRMS (FAB⁺): calcd for [M+H]⁺, 434.1157; found, 434.1155. Mp: 109–111 °C.

4.5. Mass spectrometric analysis

3-Nitrobenzyl alcohol was used as the matrix. A powder of DPPEA-HC or DPPEA-HC oxide was used in the measurement. A sample, 1 mg of DPPEA-HC dissolved in 10 μL of DMSO in the presence of 1 M H₂O₂, was used, in order to confirm that DPPEA-HC reacts with H₂O₂ to form DPPEA-HC oxide.

4.6. Fluorometric analysis

In steady-state fluorescence spectroscopic studies, the slit width was 1.5 nm for both excitation and emission. DPPEA-HC and DPPEA-HC oxide were dissolved in DMSO to produce 5 mM stock solutions for each compound. These solutions were then diluted to the required concentration for the subsequent measurements. The content of DMSO in each solution was 0.2% (v/v).

Relative quantum efficiencies of fluorescence of DPPEA-HC and DPPEA-HC oxide were obtained by comparing the area of the emission spectrum for the test sample excited at 366 nm in 100 mM sodium phosphate buffer (pH 7.4) with that for a solution of 7-hydroxycoumarin excited at the same wavelength, which has a quantum efficiency of 0.76 according to the literature.²⁴ The quantum efficiencies of fluorescence were obtained from multiple measurements (*n* = 3) with the following equation

$$\phi_{\text{sample}} = \phi_{\text{standard}} \times \frac{\text{Abs}_{\text{standard}}}{\text{Abs}_{\text{sample}}} \times \frac{\Sigma[F_{\text{sample}}]}{\Sigma[F_{\text{standard}}]}$$

where Abs and *F* denote the absorbance and fluorescence intensity, respectively, and Σ[*F*] denotes the peak area of the fluorescence spectra, calculated by summation of the fluorescence intensity.

In time-resolved fluorescence studies, the pulse width was 600 ps and the wavelengths were 337.1 nm (N₂ laser), 396 nm (dye laser for DPPEA-HC and DPPEA-HC oxide). The decay curves were analyzed by single-exponential fitting after deconvolution of the excitation light pulse profile. The goodness of the fit was judged with the reduced χ² value (<1.2 in all cases), the randomness of the residuals, and the autocorrelation function.

4.7. Computational methods

All geometry optimizations were performed using PM3,²⁵ which is available in the molecular orbital package WinMOPAC3.0 by Fujitsu Ltd. The results of the calculation were recalculated using a hybrid density functional theory (B3LYP)²⁶ with the 6-31G* basis set as implemented in Gaussian 98W.²⁷ Calculations using AM1²⁸ in WinMOPAC3.0 were subsequently carried out where the optimized structures obtained by the calculations using Gaussian 98W were maintained. In the AM1 calculation, the CIS calculation method²⁹ was used for the evaluation of the energy value at the excited state.

Acknowledgements

We wish to thank Mr. Taisuke Iseda for the measurements of mass spectra. This work was supported by a research grant from the Ministry of Education, Science, Sports and Culture of Japan (grant number; 16023249 to N.S.).

References and notes

- (a) Halliwell, B.; Gutteridge, J. M. C. *Free Radicals in Biology and Medicine*, 2nd ed.; Clarendon: New York, 1989; (b) Stamler, J. S.; Singel, D. J.; Loscalzo, J. *Science* **1992**, *158*, 1898; (c) Ames, B. N.; Shigenaga, M. K.; Hagen, T. M. *Proc. Natl. Acad. Sci. U.S.A.* **1993**, *90*, 7915.
- (a) Martin, W. J. *Am. Rev. Respir. Dis.* **1984**, *130*, 209; (b) Lewis, M. S.; Whatley, R. E.; Cain, P.; McIntyre, T. M.;

- Prescott; Zimmerman, G. A. *J. Clin. Invest.* **1988**, *82*, 2045; (c) Gasic, A. C.; McGuire, G.; Krater, S.; Farhood, A. I.; Goldstein, M. A.; Smith, C. W.; Entman, M. L.; Taylor, A. A. *Circulation* **1991**, *84*, 2154.
3. Mohazzab, H. K.; Kaminski, P. M.; Fayngersh, R. P.; Wolin, M. S. *Am. J. Physiol. Heart Circ. Physiol.* **1996**, *270*, H1044.
4. (a) Cosentino, F.; Katusic, Z. S. *Circulation* **1995**, *91*, 139; (b) Katusic, Z. S. *Am. J. Physiol. Heart Circ. Physiol.* **2001**, *281*, H981.
5. Matoba, T.; Shimokawa, H.; Nakashima, M.; Hirakawa, Y.; Mukai, Y.; Hirano, K.; Kanaide, H.; Takeshita, A. *J. Clin. Invest.* **2000**, *106*, 1521.
6. Iida, Y.; Katusic, Z. S. *Stroke* **2000**, *31*, 2224.
7. Mason, W. T.; Mason, B. T. *Fluorescent and Luminescent Probes for Biological Activity*, 2nd ed.; Academic: New York, 1999.
8. (a) Kojima, H.; Nakatsubo, N.; Kikuchi, K.; Kawahara, S.; Kirino, Y.; Nagoshi, H.; Hirata, Y.; Nagano, T. *Anal. Chem.* **1998**, *70*, 2446; (b) Kojima, H.; Hirotani, M.; Nakatsubo, N.; Kikuchi, K.; Urano, Y.; Higuchi, T.; Hirata, Y.; Nagano, T. *Anal. Chem.* **2001**, *73*, 1967; (c) Gabe, Y.; Urano, Y.; Kikuchi, K.; Kojima, H.; Nagano, T. *J. Am. Chem. Soc.* **2004**, *126*, 3357; (d) Meineke, P.; Rauen, U.; de Groot, H.; Korth, H. G.; Sustmann, R. *Biol. Chem.* **2000**, *381*, 575; (e) Meineke, P.; Rauen, U.; de Groot, H.; Korth, H. G.; Sustmann, R. *Chem. Eur. J.* **1999**, *5*, 1738; (f) Franz, K. J.; Singh, N.; Lippard, S. J. *Angew. Chem., Int. Ed.* **2000**, *39*, 2120; (g) Franz, K. J.; Singh, N.; Spingler, B.; Lippard, S. J. *Inorg. Chem.* **2000**, *39*, 4081; (h) Katayama, Y.; Soh, N.; Maeda, M. *Chemphyschem* **2001**, *2*, 101; (i) Soh, N.; Katayama, Y.; Maeda, M. *Analyst* **2001**, *126*, 564; (j) Katayama, Y.; Soh, N.; Maeda, M. *Bull. Chem. Soc. Jpn.* **2002**, *75*, 1681; (k) Soh, N.; Imato, T.; Kawamura, K.; Maeda, M.; Katayama, Y. *Chem. Commun.* **2002**, 2650.
9. (a) Nardello, V.; Azaroual, N.; Cervoise, I.; Vermeersch, G.; Aubry, J. M. *Tetrahedron* **1996**, *52*, 2031; (b) Umezawa, N.; Tanaka, K.; Urano, Y.; Kikuchi, K.; Higuchi, T.; Nagano, T. *Angew. Chem., Int. Ed.* **1999**, *38*, 2899; (c) Tanaka, K.; Miura, T.; Umezawa, N.; Urano, Y.; Kikuchi, K.; Higuchi, T.; Nagano, T. *J. Am. Chem. Soc.* **2001**, *123*, 2530.
10. (a) Makrigiorgos, G. M.; Baranowska-Kortylewicz, J.; Bump, E.; Sahu, S. K.; Berman, R. M.; Kassiss, A. I. *Int. J. Radiat. Biol.* **1993**, *63*, 445; (b) Makrigiorgos, G. M.; Folkard, M.; Huang, C.; Bump, E.; Baranowska-Kortylewicz, J.; Sahu, S. K.; Michael, B. D.; Kassiss, A. I. *Radiat. Res.* **1994**, *138*, 177; (c) Setsukinai, K.; Urano, Y.; Kakinuma, K.; Majima, H. J.; Nagano, T. *J. Biol. Chem.* **2003**, *278*, 3170; (d) Soh, N.; Makihara, K.; Sakoda, E.; Imato, T. *Chem. Commun.* **2004**, 496.
11. Royall, J. A.; Ischiropoulos, H. *Arch. Biochem. Biophys.* **1993**, *302*, 348.
12. Hempel, S. L.; Buettner, G. R.; O'Malley, Y. Q.; Wessels, D. A.; Flaherty, D. M. *Free. Radic. Biol. Med.* **1999**, *27*, 146.
13. Wolfbeis, O. S.; Dürkop, A.; Wu, M.; Lin, Z. *Angew. Chem., Int. Ed.* **2002**, *41*, 4495.
14. Miura, T.; Urano, Y.; Tanaka, K.; Nagano, T.; Ohkubo, K.; Fukuzumi, S. *J. Am. Chem. Soc.* **2003**, *125*, 8666.
15. Onoda, M.; Uchiyama, S.; Endo, A.; Tokuyama, H.; Santa, T.; Imai, K. *Org. Lett.* **2003**, *5*, 1459.
16. Pinkernell, U.; Effkemann, S.; Karst, U. *Anal. Chem.* **1997**, *69*, 3623.
17. Akasaka, K.; Ohru, H.; Meguro, H. *J. Chromatogr.* **1993**, *628*, 31.
18. de Silva, A. P.; Gunarathe, H. Q. N.; Gunnlaugsson, T.; Huxley, A. J. M.; McCoy, C. P.; Rademacher, J. T.; Rice, T. E. *Chem. Rev.* **1997**, *97*, 1515.
19. (a) Deisseroth, A.; Dounce, A. L. *Physiol. Rev.* **1970**, *50*, 319; (b) Putnam, C. D.; Arvai, A. S.; Bourne, Y.; Tainer, J. A. *J. Mol. Biol.* **2000**, *296*, 295; (c) Switala, J.; Loewen, P. C. *Arch. Biochem. Biophys.* **2002**, *401*, 145.
20. (a) Hodges, G. R.; Young, M. J.; Paul, T.; Ingold, K. U. *Free Radic. Biol. Med.* **2000**, *29*, 434; (b) Lvovich, V.; Scheeline, A. *Anal. Chem.* **1997**, *69*, 454.
21. (a) McCord, J. M.; Fridovich, I. *J. Biol. Chem.* **1969**, *244*, 6056; (b) Lawrence, G. D.; Sawyer, D. T. *Biochemistry* **1979**, *18*, 3045.
22. Kyle, M. E.; Nakae, D.; Sakaida, I.; Miccadei, S.; Farber, J. L. *J. Biol. Chem.* **1988**, *263*, 3784.
23. Barltrop, J. A.; Coyle, J. D. *Excited States in Organic Chemistry*; Wiley: London, 1975.
24. Setsukinai, K.; Urano, Y.; Kikuchi, K.; Higuchi, T.; Nagano, T. *J. Chem. Soc., Perkin Trans. 2* **2000**, 2453.
25. Stewart, J. J. P. *MOPAC 97*; Fujitsu: Tokyo, 1998.
26. (a) Becke, A. D. *J. Chem. Phys.* **1993**, *98*, 5648; (b) Lee, C.; Yang, W.; Parr, R. G. *Phys. Rev. B* **1988**, *37*, 785.
27. Frisch, A.; Frisch, M. J. *Gaussian 98*; Gaussian: Pittsburgh, 1998.
28. Dewar, M. J. S.; Zoeblich, E. G.; Healy, E. F.; Stewart, J. P. *J. Am. Chem. Soc.* **1985**, *107*, 3902.
29. Foresman, J. B.; Head-Gordon, M.; Pople, J. A.; Frisch, M. J. *J. Phys. Chem.* **1992**, *96*, 135.